Structural characterization of further high temperature superionic phases of Ag_2HgI_4 and Cu_2HgI_4

2001 J. Phys.: Condens. Matter 13 5597

(http://iopscience.iop.org/0953-8984/13/24/305)

INSTITUTE OF PHYSICS PUBLISHING JOURNAL OF PHYSICS: CONDENSED MATTER

J. Phys.: Condens. Matter **13** (2001) 5597–5610 www.iop.org/Journals/cm PII: S0953-8984(01)19126-5

Structural characterization of further high temperature superionic phases of Ag_2HgI_4 and Cu_2HgI_4

S Hull[1] **and D A Keen**[1,2]

[1] The ISIS Facility, Rutherford Appleton Laboratory, Chilton, Didcot, Oxfordshire, OX11 0QX, UK
[2] Physics Department, Oxford University, Clarendon Laboratory, Parks Road, Oxford OX1 3PU, UK

Received 14 November 2000, in final form 27 April 2001

Abstract

The high temperature crystal structure of the superionic compounds Ag_2HgI_4 and Cu_2HgI_4 has been investigated using powder neutron diffraction. In addition to the widely studied $\beta \rightarrow \alpha$ superionic transitions observed in both compounds just above ambient temperature, we have characterized the transitions to phases (labelled δ) in Ag_2HgI_4 and Cu_2HgI_4 which occur at ∼410 and ∼578 K, respectively. Prior to melting, Ag_2HgI_4 undergoes an additional transition at ∼445 K to a phase labelled ε. The crystal structure of the δ phases comprises a slightly distorted h.c.p. anion sublattice with the two cation species dynamically disordered over the octahedral and tetrahedral interstices. In ε-Ag_2HgI_4 the cations are distributed over the tetrahedral and trigonal interstices formed by a b.c.c. anion sublattice and can, therefore, be considered to be a 'cation-deficient' α-AgI-type superionic phase. The implications of these experimental findings in the wider context of the family of copper- and silver-based superionic conductors and for previous suggestions of 'unusual' behaviour of the $\alpha \leftrightarrow \delta$ transition are discussed.

1. Introduction

The high temperature crystal structures of copper (I) iodide (CuI) and silver iodide (AgI) have been extensively studied owing to their superionic behaviour, which is associated with the presence of extensive dynamic cation disorder [1]. At ambient temperature γ-CuI adopts the cubic zincblende structure (space group $F\bar{4}3m$), in which the I^- ions form a face-centred cubic (f.c.c.) array and the Cu^+ ions are ordered over half the available tetrahedral interstices [2]. AgI usually exists as a two phase mixture of the zincblende-structured γ phase and the β phase, which has the wurtzite structure (space group $P6_3mc$ and the hexagonal close-packed (h.c.p.) equivalent of the cubic zincblende arrangement) [3]. On heating, CuI transforms to its β phase at 642 K, which was originally believed to adopt the wurtzite structure [4]. However, subsequent diffraction studies showed the presence of the 001 Bragg reflection that is systematically absent in $P6_3mc$ symmetry, and other structural models in space groups $P\bar{6}m2$ [5], $P3m1$ [6] and $P\bar{3}m1$ [7] have been described. The latter is the most recent study,

0953-8984/01/245597+14$30.00

and places the I^- ions in a slightly distorted h.c.p. array with the Cu^+ ions distributed over half the tetrahedral interstices (see later). However, there is significant cation disorder and, on average, ~15% of the Cu^+ ions occupy the alternative pair of tetrahedral interstices at 655 K [7]. On further heating to 680 K, β-CuI transforms to α-CuI, in which the I^- ion sublattice reverts to f.c.c. and the Cu^+ are randomly disordered over all the tetrahedral holes [5, 8]. AgI transforms to its superionic α phase at 420 K and, by contrast, α-AgI possesses a body-centred cubic (b.c.c.) I^- array with the Ag^+ ions distributed predominantly over the tetrahedral interstices [9, 10]. The ionic conductivity of superionic α-CuI and α-AgI are extremely high ($\sigma \sim 0.1$–$2\ \Omega^{-1}\ cm^{-1}$), with a somewhat higher value for α-AgI being attributed to a greater number of tetrahedral holes being available per diffusing cation in b.c.c. (six) than f.c.c. (two) [11].

In an attempt to identify compounds with high ionic conductivities at temperatures close to ambient, numerous ternary derivatives of AgI and CuI have been synthesized and investigated [1]. Of these, Ag_2HgI_4 and Cu_2HgI_4 have received considerable attention since their superionic transitions are only marginally above ambient temperature, at 326 K and 338 K, respectively (see [12] and references therein). At ambient temperature β-Ag_2HgI_4 and β-Cu_2HgI_4 both adopt slightly distorted f.c.c. I^- arrays and the $2 \times Ag^+/Cu^+$, $1 \times Hg^{2+}$ and $1 \times$ vacancy are ordered over the tetrahedral sites occupied in a zincblende-like arrangement in two different ways (such that the space groups of β-Ag_2HgI_4 and β-Cu_2HgI_4 are $I\bar{4}$ and $I\bar{4}2m$, respectively). Despite some debate over the structure of the high temperature superionic α phases [13–17] these have recently been shown to be isostructural, with both the cation species randomly disordered over the tetrahedral (zincblende) sites [12]. The ionic conductivity of the superionic phases is, however, four to five orders of magnitude lower than α-AgI and α-CuI, since the number of available sites per diffusing ions is only 4/3.

Differential scanning calorimetry (DSC) studies of Ag_2HgI_4 and Cu_2HgI_4 have identified a further transition in both compounds at ~425 K and ~576 K, respectively [18–21]. Following Baranowski *et al* [18], we label these higher temperature phases δ. In the case of Ag_2HgI_4, the $\alpha \leftrightarrow \delta$ transition has been reported to show extraordinary behaviour as a function of pressure. The phase boundary initially increases with pressure, reaches a maximum at $p \sim 0.05$ GPa/$T = 428$ K and then falls [18–20]. However, at $p \gtrsim 0.15$ GPa the DSC measurements show no latent heat, but only a change in the specific heat, indicating that the phase transition is of second order. At $p = 0.47$ GPa/$T = 382$ K there is a tricritical point, characterized by an abrupt upturn in the $\alpha \leftrightarrow \delta$ phase boundary and a change in the character of the transition to first order. As such, this has been proposed to be an example of a change from a first-order to a second-order transition, of the type first discussed by Landau [22]. However, this assignment is rather speculative because the structural properties of the δ phases are not known. In the silver compound, δ-Ag_2HgI_4 has been proposed to adopt a b.c.c. δ-AgI-like structure or a wurtzite type β-AgI arrangement [20]. However, the possibility of thermally induced dissociation has also been proposed, especially in the case of Cu_2HgI_4 (i.e. $Cu_2HgI_4 \leftrightarrow CuI + CuHgI_3$) [23].

This paper extends our recent work on the α- and β-phases of Ag_2HgI_4 and Cu_2HgI_4 [12] and reports powder neutron diffraction studies of Ag_2HgI_4 and Cu_2HgI_4 at temperatures up to 483 K and 663 K, respectively. These are used to investigate the nature of the two $\alpha \leftrightarrow \delta$ transitions, determine the high temperature structure(s) for the first time and compare these with the parent AgI and CuI compounds.

2. Experiment

The samples of Ag_2HgI_4 and Cu_2HgI_4 used in this study were supplied by the Cerac Chemical Co. and were of stated purity 99.5%. Powder neutron diffraction data confirmed the absence

of any additional impurity phases in either sample. Diffraction experiments were performed using the Polaris powder diffractometer at the ISIS facility, UK [24]. The samples were encapsulated inside silica tubes, of approximate wall thickness 0.5 mm, and heated inside a furnace constructed of vanadium resistive heating element and heat shields. One long measurement (∼17 hours) was made within each observed phase, together with further shorter measurements to determine the thermal expansion and position of any phase transitions. It should be noted that both mercury and silver have high neutron absorption cross-sections and this, together with the disordered nature of the phases under consideration, results in data with a relatively weak Bragg signal. Data were collected using detector banks which cover the scattering angles $85^\circ < \pm 2\theta < 95^\circ$ and provide data over the d-spacing range $\sim 0.3 < d\ (\text{Å}) \lesssim 4.3$ with a resolution $\Delta d/d \sim 6 \times 10^{-3}$. Rietveld profile refinement used the program TF12LS [25], which is based on the Cambridge Crystallographic Subroutine Library [26]. In assessing the relative quality of fits to the experimental data using different structural models the usual χ^2 statistic is used, defined by

$$\chi^2 = \sum_{N_d} \frac{(I_{obs} - I_{calc})^2}{(\sigma I_{obs})^2} / (N_d - N_p).$$

N_d is the number of data points used in the fit and N_p is the number of fitted parameters. I_{obs} and I_{calc} are the observed and calculated intensities, respectively, and σI_{obs} is the estimated standard deviation on I_{obs}, derived from the counting statistics.

When investigating a disordered structure using elastic Bragg diffraction, the aim is to characterize the disorder within the average structure as effectively as possible. To do this, models with partially occupied lattice sites are often used. The shape of the ion density distribution is mimicked by the partial occupation of a collection of sites that may be too close to each other to be simultaneously occupied. It is also possible to use anisotropic displacement parameters or models based on anharmonic lattice vibrations, although these often introduce more parameters into the model. Anisotropic displacement parameters may also be used in conjunction with partially occupied lattice site models [27]. For a superionic material, all are likely to be an approximation to the true average structure since some ions are mobile. Great care is required to ensure that the data are not overanalysed and that as few structural parameters as possible are used to characterize the structure, bearing in mind the small number of Bragg reflections produced by a highly disordered crystalline material. For this reason we only use simple partially occupied lattice site models in the structural descriptions below.

3. Results

The evolution of the powder neutron diffraction patterns of Ag_2HgI_4 and Cu_2HgI_4 on increasing temperature is illustrated in figures 1 and 2, respectively. The two abrupt changes in the diffraction pattern of Ag_2HgI_4 at ∼410 K and ∼445 K and the single change in that of Cu_2HgI_4 at ∼578 K are indicative of structural phase transitions. Following previous studies [18–21], the phases at temperatures immediately above the α phases are denoted by δ-Ag_2HgI_4 and δ-Cu_2HgI_4. The further transition in Ag_2HgI_4, which has not been reported previously, is denoted by ε-Ag_2HgI_4. However, the possibility of thermally induced dissociation (i.e. $Ag_2HgI_4 \rightarrow AgHgI_3 + AgI$) cannot be ruled out at this stage and it is necessary to assign the peaks observed in the diffraction to one, or more, phases. Attempts to index the d-spacings of the observed diffraction peaks used the program TREOR90 [28].

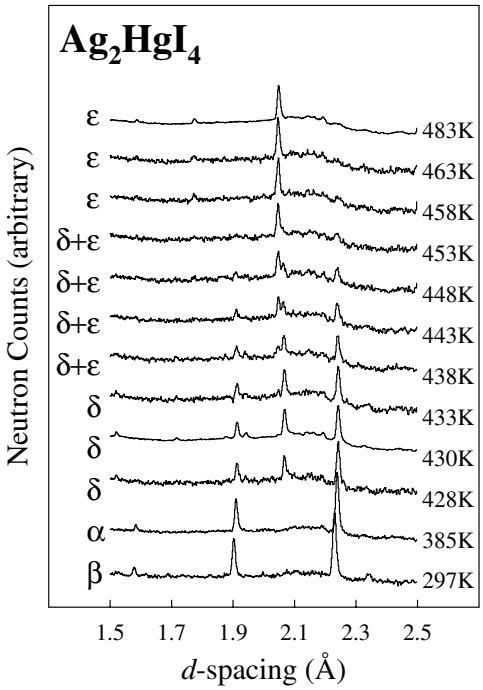

Figure 1. Plot showing the evolution of peaks in a small section of the powder neutron diffraction patterns of Ag_2HgI_4 with temperature. The $\alpha \rightarrow \delta$ transition at $T \sim 410$ K and the $\delta \rightarrow \varepsilon$ transition at $T \sim 445$ K are clearly visible.

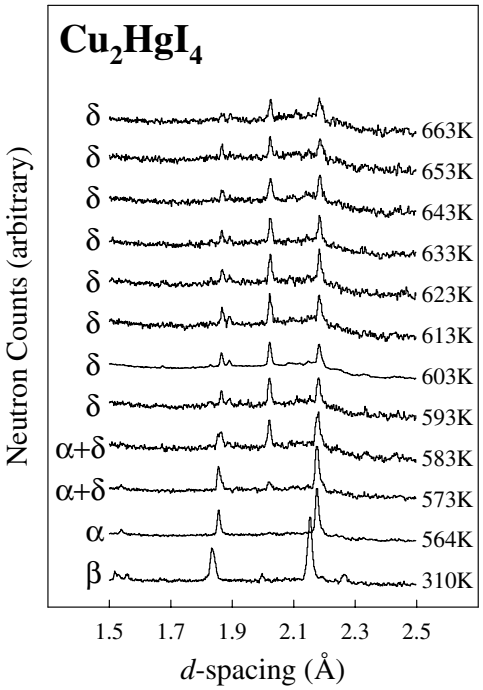

Figure 2. Plot showing the evolution of peaks in a small section of the powder neutron diffraction patterns of Cu_2HgI_4 with temperature. The $\alpha \rightarrow \delta$ transition at $T \sim 578$ K is clearly visible.

3.1. Phase δ-Ag_2HgI_4

The observed d-spacings for δ-Ag_2HgI_4 at 430(2) K can be successfully accounted for using a hexagonal unit cell of dimensions $a = 4.480$ Å and $c = 7.322$ Å. Comparison of the unit cell volume of the α-Ag_2HgI_4 phase adopted at lower temperatures indicate that this unit cell contains only half a formula unit, i.e. $1 \times Ag^+$, $\frac{1}{2} \times Hg^{2+}$ and $2 \times I^-$. Recalling that the two cation species are randomly disordered over the same crystallographic sites within α-Ag_2HgI_4 [12] it is reasonable to assume that this is also the case in the higher temperature δ phase. To confirm the assignment of the hexagonal unit cell we perform a least-squares fit to the diffraction data without imposing any structural information concerning the location of the ions. This procedure fits a polynomial describing the background scattering contribution, the unit cell constants, a Gaussian peak width parameter and the intensities of all the Bragg peaks which occur at d-spacing values consistent with the unit cell. The resultant fit indicates that all the observed Bragg peaks can be accounted for using the proposed hexagonal unit cell. It also gives a 'best possible' value for the goodness-of-fit χ^2 parameter against which the reliability of other models for the structure of δ-Ag_2HgI_4 (which impose space group symmetry and distribute the ions on specific crystallographic sites) can be assessed. In principle, it is possible to deduce the correct space group (or a small number of possible alternatives) from the systematic absence of certain classes of Bragg reflections. For the case of δ-Ag_2HgI_4, the observed reflections indicate that conditions $00l$ with l even and hhl with l even are required. These are consistent with space groups $P6_3mc$, $P\bar{6}2c$ and $P6_3/mmc$. However, given the

relatively poor peak-to-background in the measured diffraction pattern (due to the extensive lattice disorder) the selection of these three space groups in preference to other hexagonal (or trigonal) alternatives is rather inconclusive.

To determine the correct structural model for δ-Ag_2HgI_4 we note that the hexagonal unit cell has comparable dimensions to the wurtzite structure adopted by β-AgI at room temperature [2] (and by β-CuCl [29] and β-CuBr [5] at elevated temperatures) and to the trigonal structure in space group $P\bar{3}m1$ adopted by the high temperature phase β-CuI [7]. In both these modifications the anions adopt an arrangement close to hexagonal close packed (h.c.p.) and it is therefore reasonable to assume that the same is true for δ-Ag_2HgI_4. We then fit different models for the cation distribution over the various tetrahedral and octahedral voids formed by the h.c.p. anion array, initially assuming complete disorder of the Ag^+ and Hg^{2+} species. These are labelled models B to G, with model A used to denote the 'structure independent' fit described above. Crystallographic descriptions of the various models are summarized in table 1.

Table 1. The values of the goodness-of-fit parameter χ^2 (see text) obtained by least-squares fits to the diffraction data collected from δ-Ag_2HgI_4 at $T = 430(2)$ K and δ-Cu_2HgI_4 at $T = 603(2)$ K, using the structural models A to G.

				χ^2	
Model	Description	Space group	Sites	δ-Ag_2HgI_4	δ-Cu_2HgI_4
A	Intensities only	—	—	2.07	2.01
B	Octahedral sites only	$P6_3/mmc$	I^- in 2(c) at $\frac{1}{3}$, $\frac{2}{3}$, $\frac{1}{4}$, etc Ag^+/Hg^{2+} in 2(a) at 0, 0, 0, etc	28.82	19.13
C	Tetrahedral sites only	$P6_3/mmc$	I^- in 2(c) at $\frac{1}{3}$, $\frac{2}{3}$, $\frac{1}{4}$, etc Ag^+/Hg^{2+} in 4(f) at $\frac{1}{3}$, $\frac{2}{3}$, z, etc, $z \sim 5/8$	5.52	5.28
D	Octahedral and tetrahedral sites	$P6_3/mmc$	I^- in 2(c) at $\frac{1}{3}$, $\frac{2}{3}$, $\frac{1}{4}$, etc Ag^+/Hg^{2+} in 2(a) at 0, 0, 0, etc and Ag^+/Hg^{2+} in 4(f) at $\frac{1}{3}$, $\frac{2}{3}$, z, etc, $z \sim 5/8$	3.36	3.98
E	Sites M1 and M2 (see figure 3)	$P6_3mc$	I^- in 2(b) at $\frac{1}{3}$, $\frac{2}{3}$, z, etc, $z = 0$ Ag^+/Hg^{2+} in 2(b) at $\frac{1}{3}$, $\frac{2}{3}$, z, etc, $z \sim \frac{3}{8}$	~ 7.39	~ 6.68
F	Sites M1 and M3 (see figure 3)	$P\bar{6}m2$	I^- in 1(a) at 0, 0, 0 and I^- in 1(d) at $\frac{1}{3}$, $\frac{2}{3}$, $\frac{1}{2}$ Ag^+/Hg^{2+} in 2(g) 0, 0, z, etc, $z \sim \frac{3}{8}$	10.84	9.03
G	Sites M2 and M3 (see figure 3)	$P\bar{3}ml$	I^- in 2(d) at $\frac{1}{3}$, $\frac{2}{3}$, z, etc, $z \sim \frac{1}{4}$ Ag^+/Hg^{2+} in 2(d) at $\frac{1}{3}$, $\frac{2}{3}$, z, etc, $z \sim 5/8$	8.25	7.04

In space group $P6_3/mmc$ an h.c.p. anion array is formed by placing the I^- in 2(c) sites at $\frac{1}{3}$, $\frac{2}{3}$, $\frac{1}{4}$ and $\frac{2}{3}$, $\frac{1}{3}$, $\frac{3}{4}$. Model B places the cations in the octahedral voids at 2(a) 0, 0, 0 and 0, 0, $\frac{1}{2}$ whilst model C distributes them over the four tetrahedral interstices in 4(f) sites at $\frac{1}{3}$, $\frac{2}{3}$, z, etc with $z = \frac{5}{8}$. As shown in table 1, the former provides a relatively poor fit to the data with $\chi^2 = 28.8$ whilst the latter gives a reasonable fit with $\chi^2 = 5.5$. Model D distributes the cations over the octahedral and tetrahedral sites and includes an additional fitted parameter which describes the fraction of cations on the tetrahedral sites. A marked improvement to the quality of the fit over that provided by model C is obtained, with ~70% of the cations located on the tetrahedral positions.

Given the apparent preference for tetrahedral co-ordination indicated above (and also in the β and α phases [12]) models E to G constrain the cations to occupy a subset of the tetrahedral holes in the h.c.p. anion sublattice. As illustrated in figure 3, there are four tetrahedral sites

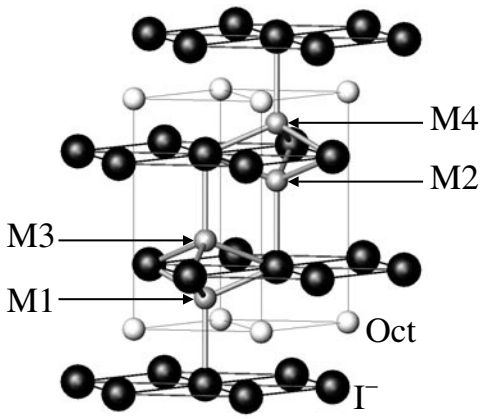

Figure 3. A schematic diagram showing the available interstitial sites within an h.c.p. sublattice (formed by the black spheres). The tetrahedral sites are shown as grey spheres and are labelled M1 to M4 (see text) whilst the octahedral sites are shown as white spheres. The narrow line indicates the unit cell.

which can accommodate, on average, $\frac{3}{2}$ cations. In α-Ag_2HgI_4 this is also true for the f.c.c. I^- sublattice and structural refinements indicate that, instead of each tetrahedral site being occupied (on average) by $\frac{3}{8}$ cations, half are occupied $\frac{3}{4}$ of the time and the other half are not involved in the conduction process [12]. To consider if the same is true for h.c.p. δ-Ag_2HgI_4, we constrain the cations to occupy pairs of tetrahedral holes. With reference to figure 3, there are three different ways to achieve this. In model E the cations only occupy the sites labelled M1 and M2. If these two sites were fully occupied then this would form the wurtzite structure [2]. Occupation of sites M1 and M3 leads to an arrangement in space group $P\bar{6}m2$ which is similar to that proposed by Bührer and Hälg for β-CuI [5], though subsequently shown to be incorrect. The correct structure of β-CuI has the cations predominantly in the sites labelled M2 and M3 [7] and this is referred to as model G. As shown in table 1, all three models give χ^2 values significantly higher than that predicted by model D (or A) and, in addition, the least-squares refinements were relatively unstable (particularly in the case of model E). Attempts to improve these fits by allowing a variable fraction of the cations to relocate to the alternate set of tetrahedral sites tended towards a situation in which all four sites were occupied to an equal extent (within error), i.e. towards model C. Occupation of only a pair of tetrahedral sites and allowing a fraction of cations to occupy the octahedral positions did not produce a significant reduction in χ^2. Finally, a number of attempts were made to investigate the possibility of ordering of the two cation species over the available sites, exploiting the significant difference between their scattering lengths ($b_{Ag} = 5.922$ fm and $b_{Hg} = 12.692$ fm [30]). However, no significant improvement in the quality of the fit was produced and we conclude that the best structural description for δ-Ag_2HgI_4 is provided by model D. The final fitted parameters are listed in table 2 and the quality of the fit is illustrated in figure 4.

3.2. Phase ε-Ag_2HgI_4

The determination of the structure of phase ε-Ag_2HgI_4 used data collected at 483(2) K. The d-spacings of the six observed reflections could be completely accounted for using a body-centred cubic lattice with $a = 5.011$ Å. This assignment was confirmed by a model independent fit to the data (referred to as model A in the summary of results for ε-Ag_2HgI_4 in table 3).

Table 2. Summary of the results of the least-squares fit to the diffraction data collected from δ-Ag_2HgI_4 at $T = 430(2)$ K.

δ-Ag_2HgI_4 $T = 430(2)$ K	
Space group	$P6_3/mmc$
Lattice parameters	$a = 4.4833(1)$ Å
	$c = 7.3252(3)$ Å
I^- in 2(c) at $\frac{1}{3}$, $\frac{2}{3}$, $\frac{1}{4}$, etc	
Isotropic thermal parameter	$B_{iso} = 6.1(2)$ Å^2
Ag^+/Hg^{2+} in 2(a) at 0, 0, 0, etc	
Isotropic thermal parameter	$B_{iso} = 18(2)$ Å^2
Site occupancy	$m = 0.47(3)$
Ag^+/Hg^{2+} in 4(f) at $\frac{1}{3}$, $\frac{2}{3}$, z, etc	
Positional parameter	$z = 0.632(1)$
Isotropic thermal parameter	$B_{iso} = 7.7(5)$ Å^2
Site occupancy	$m = 1.03(2)$
Goodness of fit	$\chi^2 = 3.36$
Weighted R-factor	$R_w = 1.55\%$
Expected R-factor	$R_{exp} = 0.85\%$
Number of data points	$N_d = 1336$
Number of Bragg peaks	$N_p = 29$
Number of Fitted parameters	$N_f = 10$

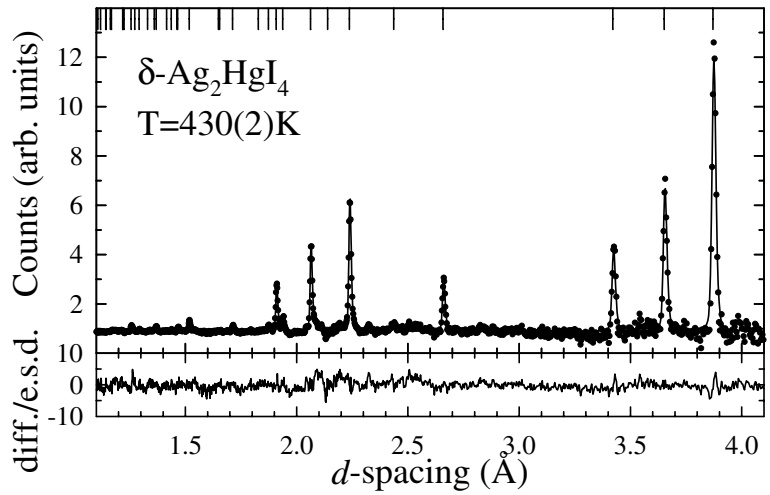

Figure 4. The final least-squares fit to the powder neutron diffraction data collected from δ-Ag_2HgI_4 at $T = 430(2)$ K. The dots are the experimental data points and the solid line is the calculated profile using the parameters listed in table 2. The lower trace shows the difference (measured minus calculated) divided by the estimated standard deviation on the experimental data points. The tick marks along the top of the figure denote the calculated positions of all the symmetry allowed Bragg reflections.

In common with δ-Ag_2HgI_4, the unit cell volume requires the inclusion of half a formula unit. The AgI–HgI_2 binary phase diagram indicates that the stability field of the superionic α phase observed in pure AgI extends to ~75% HgI_2 at ~540 K [31]. Clearly, as α-AgI adopts a

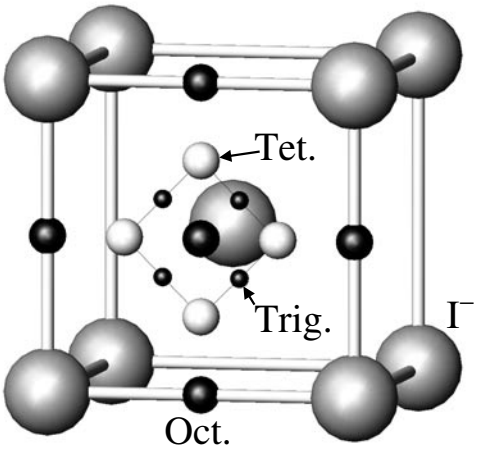

Figure 5. Schematic diagram showing the available interstitial sites within a b.c.c. sublattice (formed by the larger spheres). The octahedral, tetrahedral and trigonal sites are shown as the larger black, grey and smaller black spheres, respectively. The narrow line indicates the probable cation diffusion pathway from tetrahedral site to tetrahedral site via the trigonal positions.

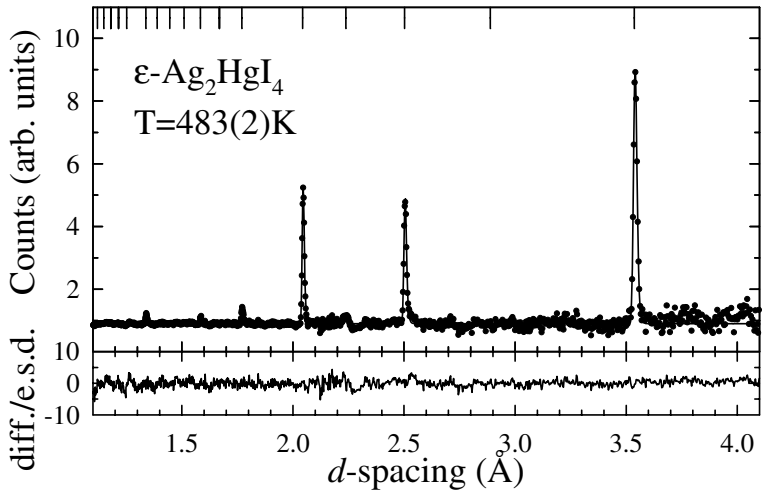

Figure 6. The final least-squares fit to the powder neutron diffraction data collected from ε-Ag_2HgI_4 at $T = 483(2)$ K. The dots are the experimental data points and the solid line is the calculated profile using the parameters listed in table 4. The lower trace shows the difference (measured minus calculated) divided by the estimated standard deviation on the experimental data points. The tick marks along the top of the figure denote the calculated positions of all the symmetry-allowed Bragg reflections.

structure in which the I^- are in a b.c.c. array (space group $Im\bar{3}m$[9, 10]) it is sensible to assume that the same is true for ε-Ag_2HgI_4. In common with the phase δ-Ag_2HgI_4 we assume that the Ag^+ and Hg^{2+} are completely disordered over various interstices formed by the anion array. With reference to table 3 and figure 5, models B to D represent attempts to locate the cations in the octahedral 6(b) sites at 0, $\frac{1}{2}$, $\frac{1}{2}$, etc, the tetrahedral 12(d) sites at $\frac{1}{4}$, 0, $\frac{1}{2}$, etc and the trigonal 24(h) $x, x, 0$ sites with $x = \frac{3}{8}$, respectively. Of these, only the latter two gave reasonable fits

Table 3. The values of the goodness-of-fit parameter χ^2 (see text) obtained by least-squares fits to the diffraction data collected from ε-Ag_2HgI_4 at $T = 483(2)$ K using the structural models A to G.

Model	Description	Space group	Sites	χ^2
A	Intensities only	—	—	1.53
B	Octahedral sites only	$Im\bar{3}m$	I^- in 2(a) at 0, 0, 0, etc. Ag^+/Hg^{2+} in 6(b) at 0, $\frac{1}{2}$, $\frac{1}{2}$, etc	6.57
C	Tetrahedral sites only	$Im\bar{3}m$	I^- in 2(a) at 0, 0, 0, etc Ag^+/Hg^{2+} in 12(d) at $\frac{1}{4}$, 0, $\frac{1}{2}$, etc	2.05
D	Trigonal sites only	$Im\bar{3}m$	I^- in 2(a) at 0, 0, 0, etc Ag^+/Hg^{2+} in 24(h) at y, y, 0, etc, $y \sim \frac{3}{8}$	2.52
E	Octahedral and tetrahedral sites	$Im\bar{3}m$	I^- in 2(a) at 0, 0, 0, etc Ag^+/Hg^{2+} in 6(b) at 0, $\frac{1}{2}$, $\frac{1}{2}$, etc and Ag^+/Hg^{2+} in 12(d) at $\frac{1}{4}$, 0, $\frac{1}{2}$, etc	1.91
F	Tetrahedral and trigonal sites	$Im\bar{3}m$	I^- in 2(a) at 0, 0, 0, etc Ag^+/Hg^{2+} in 12(d) at $\frac{1}{4}$, 0, $\frac{1}{2}$, etc and Ag^+/Hg^{2+} in 24(h) at y, y, 0, etc, $y \sim \frac{3}{8}$	1.80
G	Oct., tet. and trig. sites	$Im\bar{3}m$	I^- in 2(a) at 0, 0, 0, etc Ag^+/Hg^{2+} in 6(b) at 0, $\frac{1}{2}$, $\frac{1}{2}$, etc and Ag^+/Hg^{2+} in 12(d) at $\frac{1}{4}$, 0, $\frac{1}{2}$, etc and Ag^+/Hg^{2+} in 24(h) at y, y, 0, etc, $y \sim \frac{3}{8}$	1.80

to the diffraction data, with $\chi^2 = 2.05$ and 2.52 for models C and D, respectively. Attempts to include two sites (models E and F) and three sites (model G) simultaneously, allowing the cations to be distributed over the sites (with the constraint that the total number in the unit cell equals $\frac{3}{2}$) gave an improvement to the fit. This was especially true in the case of model F, which includes only tetrahedral and trigonal positions. In the case of model G, the refined occupancy of the octahedral sites was zero within error ($m_{oct} = 0.1(2)$) and thus equivalent to model F. We therefore conclude that phase ε-Ag_2HgI_4 comprises a b.c.c. anion sublattice with approximately half of the cations occupying the tetrahedral sites and the remainder lying close to the trigonal positions. Figure 6 and table 4 illustrate the quality of the least-squares fit to the experimental data and a list of the fitted parameters, respectively.

The structure of ε-Ag_2HgI_4 shows a very close similarity to that of α-AgI reported elsewhere [9, 10] and this is consistent with the AgI–HgI_2 binary phase diagram determined by D.T.A. methods [31]. The cation occupancy of the tetrahedral and trigonal sites can be interpreted as rapid diffusion of the cations between the tetrahedral positions via the trigonal ones (see figure 5). In comparing α-AgI with ε-Ag_2HgI_4 it is important to note that the latter is 'cation deficient', i.e. there is only $\frac{3}{4}$ mobile cation per immobile one. This leads to a reduction in the unit cell volume (when scaled to the number of iodine ions the unit cell volume of ε-Ag_2HgI_4 is approximately 2.7% smaller), indicating that the lower number density of cations outweighs the stronger Coulomb repulsion between the divalent cations. No chemical dissociation was observed at any of the temperatures measured and, on cooling, the same β-phase structure was recovered.

3.3. Phase δ-Cu_2HgI_4

The marked similarity between the diffraction patterns for phase δ-Cu_2HgI_4 collected at $T = 603(2)$ K and that for δ-Ag_2HgI_4 collected at $T = 430(2)$ K suggest that they are isostructural. The successful indexing of the d-spacings of the observed reflections from

Table 4. Summary of the results of the least-squares fit to the diffraction data collected from ε-Ag_2HgI_4 at $T = 483(2)$ K.

ε-Ag_2HgI_4 $T = 483(2)$ K	
Space group	$Im\bar{3}m$
Lattice parameter	$a = 5.015\,99(9)$ Å
I^- in 2(a) at 0, 0, 0, etc	
Isotropic thermal parameter	$B_{iso} = 4.9(4)$ Å^2
Ag^+/Hg^{2+} in 12(d) at $\frac{1}{4}$, 0, $\frac{1}{2}$, etc	
Isotropic thermal parameter	$B_{iso} = 6.9(3)$ Å^2
Site occupancy	$m = 0.77(5)$
Ag^+/Hg^{2+} in 24(h) at y, y, 0, etc	
Positional parameter	$y = 0.383(2)$
Isotropic thermal parameter	$B_{iso} = 6.9(3)$ Å^2
Site occupancy	$m = 0.73(5)$
Goodness of fit	$\chi^2 = 1.80$
Weighted R-factor	$R_w = 1.17\%$
Expected R-factor	$R_{exp} = 0.87\%$
Number of data points	$N_d = 1328$
Number of Bragg peaks	$N_p = 11$
Number of fitted parameters	$N_f = 8$

Table 5. Summary of the results of the least-squares fit to the diffraction data collected from δ-Cu_2HgI_4 at $T = 603(2)$ K.

δ-Cu_2HgI_4 $T = 603(2)$ K	
Space group	$P6_3/mmc$
Lattice parameters	$a = 4.3640(2)$ Å
	$c = 7.1759(3)$ Å
I^- in 2(c) at $\frac{1}{3}$, $\frac{2}{3}$, $\frac{1}{4}$, etc	
Isotropic thermal parameter	$B_{iso} = 4.2(2)$ Å^2
Cu^+/Hg^{2+} in 2(a) at 0, 0, 0, etc	
Isotropic thermal parameter	$B_{iso} = 8(2)$ Å^2
Site occupancy	$m = 0.68(3)$
Cu^+/Hg^{2+} in 4(f) at $\frac{1}{3}$, $\frac{2}{3}$, z, etc	
Positional parameter	$z = 0.630(2)$
Isotropic thermal parameter	$B_{iso} = 4.3(5)$ Å^2
Site occupancy	$m = 0.82(3)$
Goodness of fit	$\chi^2 = 3.98$
Weighted R-factor	$R_w = 1.64\%$
Expected R-factor	$R_{exp} = 0.82\%$
Number of data points	$N_d = 1336$
Number of Bragg peaks	$N_p = 28$
Number of Fitted parameters	$N_f = 10$

δ-Cu_2HgI_4 using a hexagonal unit cell with $a = 4.365$ Å and $c = 7.172$ Å supports this assumption and our attempts to derive its structure closely followed those described in section 3.1 for δ-Ag_2HgI_4. A summary of the results obtained by fitting the diffraction data is given in table 1. In common with δ-Ag_2HgI_4, the best fit to the data is obtained using the

structural model D, which distributes the cations over all the tetrahedral and octahedral sites. The values of its fitted parameters are listed in table 5 and the quality of the fit is illustrated in figure 7.

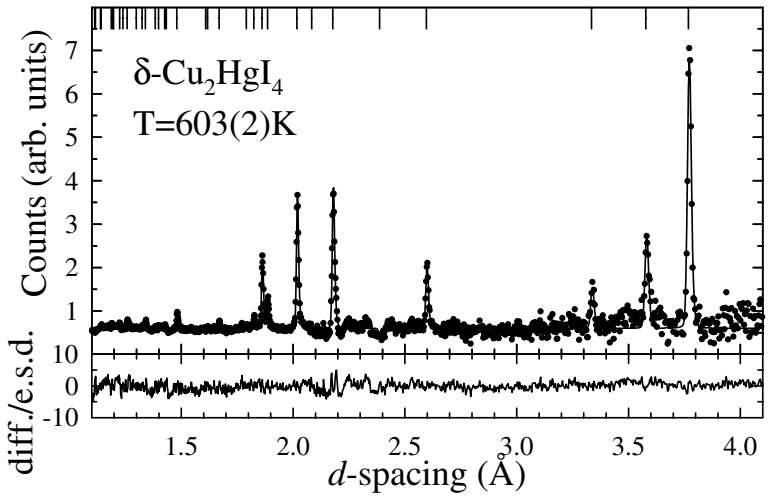

Figure 7. The final least-squares fit to the powder neutron diffraction data collected from δ-Cu_2HgI_4 at $T = 603(2)$ K. The dots are the experimental data points and the solid line is the calculated profile using the parameters listed in table 5. The lower trace shows the difference (measured minus calculated) divided by the estimated standard deviation on the experimental data points. The tick marks along the top of the figure denote the calculated positions of all the symmetry-allowed Bragg reflections.

3.4. Further high temperature phases of Cu_2HgI_4

In agreement with the binary CuI–HgI_2 phase diagram [32], there is no high temperature ε phase in Cu_2HgI_4 which might, by analogy with Ag_2HgI_4, be expected to adopt an f.c.c. superionic structure of the type found in α-CuI. However, the absence of such a phase may be due to cation size effects, the relative similarity in the radii of Ag^+ and Hg^{2+} ($r_{Ag^+} = 1.01$ Å, $r_{Hg^{2+}} = 0.96$ Å [33]) being more conducive to solid solution formation that its Cu^+ counterpart ($r_{Cu^+} = 0.60$ Å [33]). In addition, at the highest temperature measured, the sample melted, and there was no indication of chemical dissociation. After the experiment, the β-phase of Cu_2HgI_4 was recovered at room temperature.

4. Discussion

As discussed in section 3.1, the time-averaged structures of the phases δ-Ag_2HgI_4 and δ-Cu_2HgI_4 comprise a slightly distorted h.c.p. anion sublattice. This would display ideal 12-fold co-ordination if the ratio of the unit cell axes $c/a = \sqrt{8/3} = 1.6330$. In the case of δ-Ag_2HgI_4 the results presented in table 2 indicate that $c/a = 1.6339(1)$, so that the anion sublattice is extremely close to an undistorted h.c.p. array. For δ-Cu_2HgI_4, table 5 shows that $c/a = 1.6443(1)$, again close to an ideal h.c.p. array, and there are six I^-–I^- distances of 4.364 Å and a further six of 4.384 Å. In both materials c/a does not change significantly with temperature.

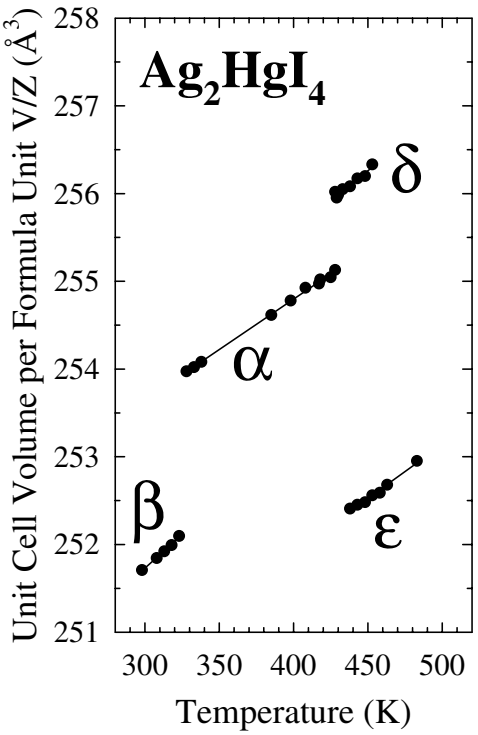

Figure 8. The temperature variation of the unit cell volume per formula unit (V/Z) of Ag_2HgI_4.

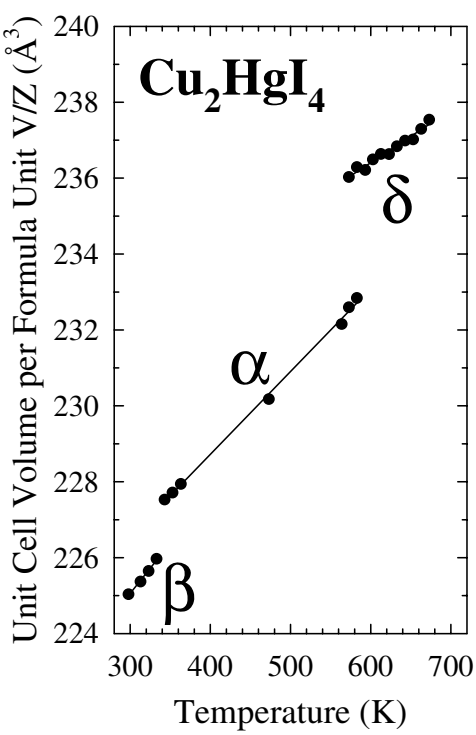

Figure 9. The temperature variation of the unit cell volume per formula unit (V/Z) of Cu_2HgI_4.

The closest related structure within one of the parent binary compounds is β-CuI, which has a rather more distorted h.c.p. anion sublattice ($c/a = 1.6693(1)$ at 665 K [7]). However, the major distinction lies in the Cu^+ distribution. In β-CuI approximately 85% of the cations are ordered onto one of the pairs of tetrahedral interstices with the remainder on the alternative pair of sites. β-CuI therefore shows only limited disorder and, whilst its ionic conductivity is relatively high ($\sigma \sim 0.03\ \Omega^{-1}\ cm^{-1}$ [34]), it does not exhibit completely random disorder of a mobile ion over a (larger) number of similar crystallographic sites and is not, therefore, a 'true' superionic phase. In the case of an f.c.c. sublattice (such as α-CuI) there are two tetrahedral sites available per immobile ion. Whilst the same is true for h.c.p., two of the tetrahedral sites (for example M1 and M3 in figure 3) are sufficiently close that they cannot be occupied simultaneously. In the case of β-CuI, the number of available tetrahedral sites therefore equals the number of mobile cations and this is likely to hinder the development of 'true' superionic behaviour. However, in the case of δ-Ag_2HgI_4 and δ-Cu_2HgI_4 the ratio of mobile to immobile ions is 3:4 and superionic behaviour is thus favoured. The cations within the δ phases of Ag_2HgI_4 and Cu_2HgI_4 are distributed predominantly over all the tetrahedral 4(f) sites of space group $P6_3/mmc$ though a significant fraction occupy the 2(a) octahedral positions. The latter is somewhat unexpected, given the preference of Ag^+ and Cu^+ for tetrahedral co-ordination in the other superionic halide phases [5, 7–10, 12, 35–37] and the preference of Hg^{2+} for tetrahedral co-ordination within its ambient temperature HgI_2 structure [2]. One possibility is that the octahedral site is not a stable minimum for the cations but the presence of significant scattering density at these positions is indicative of cations diffusing from tetrahedral to tetrahedral

sites through the octahedral positions. The uncertainty about whether an interstitial site is occupied or not has been discussed in the context of a number of other superionic systems, including α-CuI, where depending on the exact definition of site occupancy, the octahedral site is described as 'occupied' [38] or 'unoccupied' [39]. Clearly, modelling studies are required to establish details of the diffusion process at the ionic level.

Since the α-phases of Ag_2HgI_4 and Cu_2HgI_4 are superionic, it is very likely that the higher temperature δ- and ε-phases are also superionic. The $\alpha \rightarrow \delta$ and $\delta \rightarrow \varepsilon$ transitions in Ag_2HgI_4 and the $\alpha \rightarrow \delta$ transition in Cu_2HgI_4 are therefore examples of structural transitions between two superionic phases in which the arrangement of the immobile lattice changes. There are relatively few examples of this type of behaviour, the f.c.c. to b.c.c. ($\alpha \rightarrow \gamma$) transition in Ag_2Te and the b.c.c. to f.c.c. ($\beta \rightarrow \alpha$) transition in Ag_2S having been reported elsewhere [40–42]. In principle, such transitions allow the influence of the structure of the immobile sublattice on the ionic conductivity process to be investigated, providing that high temperature ionic conductivity data are available. We intend to follow this structural investigation with impedance spectroscopy measurements in the near future.

In some senses, the sequence of phase transitions in Ag_2HgI_4 is more similar to that observed in CuBr, which passes through zincblende (γ), wurtzite (β) and α-AgI bcc (α) structures on heating [5, 43]. The difference in the two compounds relates to the increased disorder and reduced number of mobile to immobile ions in Ag_2HgI_4 giving rise to higher conductivity in f.c.c. α-Ag_2HgI_4 than γ-CuBr. By a similar analogy, it could be argued that Cu_2HgI_4 mimics CuCl, and the application of modest pressure may form a b.c.c. phase of Cu_2HgI_4 [36].

Finally, the 'unusual' nature of the $\alpha \rightarrow \delta$ transition in Ag_2HgI_4 and Cu_2HgI_4 has motivated a number of previous studies [18–21]. However, this work shows unambiguously that the transition is a straightforward structural phase transformation. Consideration of the temperature variation of the unit cell volume per formula unit for Ag_2HgI_4 and Cu_2HgI_4 (figures 8 and 9, respectively) shows that the $\alpha \rightarrow \delta$ transition is accompanied by volume increases of 0.35% and 1.47%, respectively, and is, therefore, of first order. As such, it is difficult to reconcile these results with the previous observations that the $\alpha \rightarrow \delta$ transitions becomes second-order under pressure, though clearly it is necessary to perform diffraction studies in the relevant region of p-T space to clarify the situation.

5. Conclusions

Three further high temperature phases of Ag_2HgI_4 and Cu_2HgI_4 have been identified and fully characterized for the first time using powder neutron diffraction. These phases, which exist at temperatures above the known superionic α-phases, possess structures that are typical of many copper and silver superionic compounds. As a result, these two compounds may now be placed correctly within this family of superionic compounds. The present measurements further endorse the idea that the α-AgI b.c.c. structure is ubiquitous within the silver- and copper-based family of superionic conductors. It has been observed in AgI [9, 10], CuI [37], CuBr [5, 43] and CuCl [36] (cation:anion ratio of 1), Ag_3Si [27] (ratio 1.5), Ag_2S [44] Ag_2Se [45] and Ag_2Te [40, 41] (ratio 2) and now in Ag_2HgI_4 (ratio 0.75). Given the appropriate conditions of temperature and pressure there is enormous preference for the formation of this structure.

Acknowledgments

The work presented in this paper forms part of a wider project investigating the structural properties of superionic conductors funded by the Engineering and Physical Sciences Research Council (reference GR/M38711).

References

[1] Chandra S 1981 *Superionic Solids. Principles and Applications* (Amsterdam: North-Holland)
[2] Wyckoff R W G 1963 *Crystal Structures* vol 1 (New York: Wiley–Interscience)
[3] Burley G 1967 *Acta Crystallogr.* **23** 1
[4] Miyake S, Hoshino S and Takenaka T 1952 *J. Phys. Soc. Japan* **7** 19
[5] Bührer W and Hälg W 1977 *Electrochim. Acta* **22** 701
[6] Sakuma T 1988 *J. Phys. Soc. Japan* **57** 565
[7] Keen D A and Hull S 1994 *J. Phys.: Condens. Matter* **6** 1637
[8] Keen D A and Hull S 1995 *J. Phys.: Condens. Matter* **7** 5793
[9] Wright A F and Fender B E F 1977 *J. Phys. C: Solid State Phys.* **10** 2261
[10] Nield V M, Keen D A, Hayes W and McGreevy R L 1993 *Solid State Ion.* **66** 247
[11] Boyce J B and Huberman B A 1979 *Phys. Rep.* **51** 189
[12] Hull S and Keen D A 2000 *J. Phys.: Condens. Matter* **12** 3751
[13] Ketelaar J A A A 1934 *Z. Kristallogr.* **87** 436
[14] Kasper J S and Browall K W 1975 *J. Solid State Chem.* **13** 49
[15] Berthold H J and Kaese P M 1989 *Z. Kristallogr.* **186** 40
[16] Hibma T, Beyeler H U and Zeller H R 1976 *J. Phys. C: Solid State Phys.* **9** 1691
[17] Eriksson L, Wang P and Werner P-E 1991 *Z. Kristallogr.* **197** 235
[18] Baranowski B, Friesel M and Lundén A 1986 *Physica* B **139/140** 263
[19] Baranowski B, Friesel M and Lundén A 1986 *Phys. Rev.* B **33** 7753
[20] Baranowski B, Friesel M and Lundén A 1988 *Solid State Ion.* **28–30** 194
[21] Friesel M, Baranowski B and Lundén A 1987 *Phys. Scr.* **35** 34
[22] Landau L 1935 *Physik. Z. Sowjetunion* **8** 113
[23] Heintz E A 1961 *J. Inorg. Nucl. Chem.* **21** 64
[24] Hull S, Smith R I, David W I F, Hannon A C, Mayers J and Cywinski R 1992 *Physica* B **180/181** 1000
[25] David W I F, Ibberson R M and Matthewman J C 1992 *Rutherford Appleton Laboratory Report* RAL-92-032
[26] Brown P J and Matthewman J C 1987 *Rutherford Appleton Laboratory Report* RAL-87-010
[27] Hull S, Keen D A, Gardner N J G and Hayes W 2001 *J. Phys.: Condens. Matter* **13** 2295
[28] Werner P-E, Eriksson L and Westdahl M 1985 *J. Appl. Crystallogr.* **18** 367
[29] Altorfer F, Graneli B, Fischer P and Bührer W 1994 *J. Phys.: Condens. Matter* **6** 9949
[30] Sears V F 1992 *Neutron News* **3** 26
[31] Otsubo Y, Nitta A, Kaneko M, Iwata Y and Ueki A 1966 *J. Chem. Soc. Japan: Indust. Chem.* **69** 1716
[32] Nölting J, Wiegert F and Puschmann E 1989 *Ber. Bunsenges. Phys. Chem.* **93** 1335
[33] Shannon R D 1976 *Acta Crystallogr.* A **32** 751
[34] Matsui T and Wagner J B 1977 *J. Electrochem. Soc.* **124** 300
[35] Keen D A, Hull S, Hayes W and Gardner N J G 1996 *Phys. Rev. Lett.* **77** 4914
[36] Hull S and Keen D A 1996 *J. Phys.: Condens. Matter* **8** 619
[37] Hull S, Keen D A, Hayes W and Gardner N J G 1998 *J. Phys.: Condens. Matter* **10** 10 941
[38] Ihata K and Okazaki H 1997 *J. Phys.: Condens. Matter* **9** 1477
[39] Zheng-Johansson J X M, Ebbsjö I and McGreevy R L 1996 *Solid State Ion.* **83** 35
[40] Schneider J and Schulz H 1993 *Z. Kristallogr* **203** 1
[41] Keen D A and Hull S 1998 *J. Phys.: Condens. Matter* **10** 8217
[42] Miyatani S 1981 *J. Phys. Soc. Japan* **50** 3415
[43] Nield V M, McGreevy R L, Keen D A and Hayes W 1994 *Physica* B **202** 159
[44] Cava R J, Reidinger F and Wuensch B J 1980 *J. Solid State Chem.* **31** 69
[45] Rino J P, Hornos Y M M, Antonio G A, Ebbsjö I, Kalia R K and Vashishta P 1988 *J. Chem. Phys.* **89** 7542